EFFECT OF BOUNDARY LAYER ON THRUST DEDUCTION

by

S. P. G. Dinavahi & L. Landweber

sponsored by

The Naval Ship Systems Command
General Hydromechanics Research Program
administered by
The David Taylor Naval Ship Research & Development Center
with Contract N00014-79-C-0243

IIHR Report No. 239

Iowa Institute of Hydraulic Research
The University of Iowa
Iowa City, Iowa 52242

November 1981

EFFECT OF BOUNDARY LAYER ON THRUST DEDUCTION

by

S. P. G. Dinavahi & L. Landweber

sponsored by

The Naval Ship Systems Command
General Hydromechanics Research Program
administered by
The David Taylor Naval Ship Research & Development Center
with Contract N00014-79-C-0243

IIHR Report No. 239

Iowa Institute of Hydraulic Research
The University of Iowa
Iowa City, Iowa 52242

November 1981

Unclassified

SECURITY CLASSIFICATION OF THIS PAGE (When Data Entered)

REPORT DOCUMENTATION PAGE		READ INSTRUCTIONS BEFORE COMPLETING FORM
1. REPORT NUMBER IIHR Report #239	2. GOVT ACCESSION NO. A119 799	3. RECIPIENT'S CATALOG NUMBER
4. TITLE (and Subtitle) EFFECT OF BOUNDARY LAYER ON THRUST DEDUCTION		5. TYPE OF REPORT & PERIOD COVERED Final Report Oct. 1978-Oct. 1980 6. PERFORMING ORG. REPORT NUMBER
7. AUTHOR(s) S.P.G. Dinavahi and L. Landweber		8. CONTRACT OR GRANT NUMBER(s) N00014-79-C-0243
9. PERFORMING ORGANIZATION NAME AND ADDRESS Iowa Institute of Hydraulic Research The University of Iowa Iowa City, Iowa 52242		10. PROGRAM ELEMENT, PROJECT, TASK AREA & WORK UNIT NUMBERS
11. CONTROLLING OFFICE NAME AND ADDRESS David Taylor Naval Ship Research & Development Center, Bethesda, Maryland 20084		12. REPORT DATE November 1981 13. NUMBER OF PAGES 49
14. MONITORING AGENCY NAME & ADDRESS(if different from Controlling Office) Same as 11		15. SECURITY CLASS. (of this Report) Unclassified 15a. DECLASSIFICATION/DOWNGRADING SCHEDULE

16. DISTRIBUTION STATEMENT (of this Report)

Approved for public release; distribution unlimited

17. DISTRIBUTION STATEMENT (of the abstract entered in Block 20, if different from Report)

Same as 16

18. SUPPLEMENTARY NOTES

19. KEY WORDS (Continue on reverse side if necessary and identify by block number)

Thrust deduction; irrotational flow; boundary layer

20. ABSTRACT (Continue on reverse side if necessary and identify by block number)

Methods of computing thrust deduction usually ignore viscous effects and assume that the flow field of the ship and propeller is irrotational. The present work was undertaken in order to compare the computed values of the thrust deduction with and without the boundary layer and wake. A streamlined body of revolution was selected, and a sink on the axis behind the body was used as a simple mechanism to simulate the suction at the stern induced by a propeller.

DD FORM 1 JAN 73 1473 EDITION OF 1 NOV 65 IS OBSOLETE
S/N 0102-014-6601 |

Unclassified
SECURITY CLASSIFICATION OF THIS PAGE (When Data Entered)

A measure of the accuracy of a calculated irrotational-flow pressure distribution for a body in a uniform stream is the nonzero magnitude of its pressure drag. It has been found that, for calculating thrust deduction, the errors of available methods were unacceptably large. A procedure for obtaining greatly increased accuracy was developed and applied to calculate the thrust deduction for irrotational flow.

When the boundary layer and wake are present, the thick boundary near the tail of the body is first calculated by a previously developed method in which the equation of a thick boundary layer and wake are solved numerically by finite differences, and the outer irrotational flow is obtained as the solution of an integral equation. An iteration procedure in which the inner and outer flows are successively adjusted converges to the desired solution. It was found that results obtained in the wake were not sufficiently accurate, so that a momentum analysis using a special control volume was used to calculate the viscous drag with and without the sink.

The calculated values of the thrust deduction are $C_D = 0.00021$ from irrotational flow and 0.00043 from the boundary-layer potential-flow interaction method. These are tentative results until the development of an improved procedure for calculating the thick boundary layer and wake, which is underway, has been completed.

ABSTRACT

Methods of computing thrust deduction usually ignore viscous effects and assume that the flow field of the ship and propeller is irrotational. The present work was undertaken in order to compare the computed values of the thrust deduction with and without the boundary layer and wake. A streamlined body of revolution was selected, and a sink on the axis behind the body was used as a simple mechanism to simulate the suction at the stern induced by the propeller.

A measure of the accuracy of a calculated irrotational-flow pressure distribution for a body in a uniform stream is the nonzero magnitude of its pressure drag. It has been found that, for calculating thrust deduction, the errors of available methods were unacceptably large. A procedure for obtaining greatly increased accuracy was developed and applied to calculate the thrust deduction for irrotational flow.

When the boundary layer and wake are present, the thick boundary near the tail of the body is first calculated by a previously developed method, in which the equations of a thick boundary layer and wake are solved numerically by finite differences, and the outer irrotational flow is obtained as the solution of an integral equation. An iteration procedure in which the inner and outer flows are successively adjusted converges to the desired solution. It was found that results obtained in the wake were not sufficiently accurate, so that a momentum analysis using a special control volume was used to calculate the viscous drag with and without the sink.

The calculated values of the thrust deduction are $C_D = 0.00021$ from irrotational flow and 0.00043 from the boundary-layer potential-flow interaction method. These are tentative results until the development of an improved procedure for calculating the thick boundary layer and wake, which is underway, has been completed.

LIST OF SYMBOLS

a	length of the elliptic nose
a_1	structure parameter $(= -\frac{\overline{uv}}{q^2})$
b	maximum radius of the body
C_D	drag coefficient $(= \frac{D}{1/2\rho U_\infty^2 S})$
C_p	pressure coefficient $(= \frac{p-p_\infty}{1/2\rho U_\infty^2})$
d	maximum diameter of the body
dS	elemental area
ds	elemental arc length
D	drag force
D_Q	$\sqrt{f^2 + 4ff'}$
e	extra rate of strain
e_{eff}	effective rate of strain
$E(K), E$	elliptic integral of second kind
EBLW	edge of the boundary layer and wake
f	$(=r^2)$ equation of the body
FMB	fixed matching boundary enclosing boundary layer and wake
G	diffusion function
h_1	longitudinal metric coefficient
I_1, I_2, I_3	integrals
K	longitudinal curvature
$K(k), K$	elliptic integral of first kind
(ℓ, m, n)	direction cosines of the normal
ℓ	length of arc from nose to tail along a meridian
ℓ_o	mixing length scale with no extra rate of strain

$\ell(y/\delta)$	mixing length
L	body length
M	strength of the sink
M'	non-dimensional strength of the sink $\frac{M}{U_\infty d^2}$
$\bar{n}$	normal vector
P	pressure and also perimeter measured along a meridian from nose to tail
P'	a point on the body such that PP' is normal to the body
p_∞	pressure at infinity
$Q(\xi,\eta,\zeta)$	a variable point on the body surface
r, r_Q, r_b	body ordinate
R	distance between the points (t,0) and (x,r)
R_{PQ}	distance between the points P and Q
R_{VP}	viscous pressure resistance
R_s	distance between the sink $(x_s,0)$ and the point (ξ,η,ζ)
R'	$\sqrt{(x-\xi)^2 + (r_P + r_Q)^2}$
R'_{PQ}	distance between the points P and Q when they are in the same meridian
s	arc length measured from nose
S	body surface
S_F	surface of the fixed matching boundary
(t,0)	point on the axis
u_s	velocity along s
u_{1s}	external potential flow velocity along s continued into boundary layer
U_∞	velocity of the approach stream
U	tangential velocity on the body surface

$\overline{uv}$	Reynolds shear stress
V	velocity along the normal n
$\bar{V}_s, \bar{V}_p$	velocity vector at a point due to the sink and its image system
(x,r,θ)	cylindrical coordinate system
α	angle made by the tangent with the α-axis
γ	strength of the vortex sheet
δ	boundary layer thickness
Δ_1	mass deficit thickness
Δ_2	momentum thickness
ρ	fluid density
τ	shear stress
ϕ	disturbance velocity potential
ϕ_d	velocity potential of a doublet
ϕ_o	ambient undisturbed velocity potential
ϕ_P	velocity potential at a point P in the field due to the sink and its image system within the body
ϕ_Q	velocity potential at a point Q on the body surface due to the sink and its image system within the body
ϕ_s	velocity potential of the sink
Φ	total velocity potential
ψ, ψ_d, ψ_o, Ψ	stream functions corresponding to ϕ, ϕ_d, ϕ_o and Φ, respectively

CHAPTER I

INTRODUCTION

For a self-propelled ship, the pressure in the stern region is reduced relative to that for a towed model because the propeller tends to accelerate the water flowing into it. Due to this action of the propeller, the forward component of the pressure is reduced, increasing the resistance experienced by the ship, and so also the thrust necessary to propel the ship. It is found in model work that if the resistance of a hull when towed at the speed V is R, the thrust necessary to propel the ship at the same speed V is greater than R and this increase in resistance is called the 'augment of resistance'. The common practice is to look upon this increase in resistance as a deduction from the thrust provided by the propeller, so that, although the propeller provides a thrust of T, tons, only R tons are available to overcome the resistance. This loss of thrust (T-R), when expressed as a fraction of the thrust T is called "the thrust deduction fraction, t" where

$$t = (T-R)/T = 1 - R/T.$$

In a recent investigation by Huang et al [1], one of the conclusions was that "Potential-Flow Propeller-Hull interaction methods predict thrust deduction and propeller-induced pressure distribution very well." The potential-flow methods used in [1] are based on the well-known

and widely used computer program of Hess and Smith [2]. It was found that the pressure drag, for irrotational flow without propeller, deviates from the theoretical value of zero by an amount of the same order of magnitude as the viscous pressure drag, R_{VP}. This drag error is a measure of the accuracy of that computer program. Nevertheless, the H.-S. method was also used to compute the pressure distribution and pressure drag with propeller, and the difference between the so-computed pressure drags was assumed to give the thrust deduction. Also, it is known that the thrust deduction is of the same order of magnitude as the viscous pressure drag, R_{VP}, and hence this method of computing thrust deduction could lead to large percentage errors. The validation of theoretical procedures of [1] requires an irrotational-flow calculation method more accurate by at least an order of magnitude than that of H.-S. to resolve the small difference between propeller thrust and viscous pressure resistance.

In order to determine the thrust deduction when the boundary layer and near wake are taken into account, it is necessary to calculate the flow characteristics under these conditions, with and without a flow-producing mechanism simulating the presence of a propeller. For accomplishing this, it was proposed to make use of a computer program for calculating the thick boundary layer by a differential method. Such a program, developed by Lee and Patel [3] for axisymmetric flow past a body of revolution, was available, but some modifications were required for the present purpose. Regarding the irrotational flow calculations, L. Landweber and D.H. Choi have developed a program which calculates the velocity distribution on the surface of the body to the required accuracy for drag

calculations. Thus the means for calculating thrust deduction for a body of revolution by irrotational-flow methods and from the boundary-layer equations were at hand. Hence this investigation to confirm the validity of the irrotational-flow procedure was undertaken.

It is proposed, first, to solve the thick boundary-layer equations for uniform flow past the body by a differential method [3] to find the drag of the body. Next the thick boundary-layer equations will be solved to find the drag with a mechanism representing the effect of the propeller. The outer irrotational-flow equations will be rederived in Chapter III with an additional singularity representing the effect of the propeller.

CHAPTER II

SELECTION OF FORM AND SINGULARITY

The thick-boundary-layer equations, when used to compute the boundary-layer characteristics for the modified spheroid [3], broke down at a point where there is discontinuity in the surface curvature. In order to resolve this problem, a more detailed analysis of the Reynolds equations is required. Hence a streamlined body of revolution with continuous slope and curvature was selected. The shape adopted is the EPH form, so-called because of its elliptical nose, parabolic after body, and hyperbolic tail. This was proposed by L. Landweber, and adopted in about 1945, as a cavitation resistant, low-drag strut for the U.S. Navy. The equation of the form, in cylindrical coordinates (x,r), is

$$r = b\left(1 - \frac{x^2}{a^2}\right)^{1/2}, \qquad (-a \leq x \leq 0)$$

$$r = b\left(1 - \frac{x^2}{2a^2}\right), \qquad (0 \leq x \leq a)$$

$$r = \frac{b}{2}\left(7 - \frac{8x}{a} + \frac{2x^2}{a^2}\right)^{1/2}, \qquad \left(a \leq x \leq a\left(2 - \frac{1}{\sqrt{2}}\right)\right)$$

with a/b = 5.5 and L/2b = 6.3055. Here a is the length of the elliptical nose, b is half the maximum diameter of the body and L is its overall length. See fig. 1.1.

1. Selection of Mechanism to Represent a Propeller

It is common practice to use a sink disc behind the tail in order to represent the propeller. For the present purpose, however, a sink was chosen in order to simplify calculations, since our purpose is to investigate a principle, rather than to perform a design calculation. The position and strength of the sink can be selected to match the thrust deduction of the propeller.

The position of the sink on the axis behind the tail is chosen arbitrarily at half the maximum beam from the tail. Having fixed the position of the sink, it now remains to determine the strength of the sink that gives the required pressure drag in potential flow, i.e., the calculated thrust deduction. For this, the drag coefficient C_D is calculated by integration of the pressure on the body surface and an expression for C_D in terms of the strength M of the sink is obtained.

The pressure drag D in irrotational flow, in which there is a uniform stream of unit velocity past the body and a sink of strength M on the axis behind the tail, is given by

$$D = \int_0^L p \, 2\pi r \, \frac{dr}{dx} \, dx \tag{2.1}$$

where p is the pressure on the surface of the body, and r is its ordinate. This may also be written as

$$D = \pi \int_0^L (p-p_\infty) \, \frac{d(r^2)}{dx} \, dx \tag{2.2}$$

where p_∞ denotes the pressure at infinity. If we define $C_D = 2D/(\rho U_\infty^2 A)$ and $C_p = 2(p-p_\infty)/\rho U_\infty^2$ where U_∞ is the free-stream velocity, A is the maximum cross-sectional area $\pi d^2/4$, and d is the maximum diameter, then equation (2.2) can be written as

$$C_D = \frac{4}{d^2} \int_0^L C_p \frac{d(r^2)}{dx} dx \tag{2.3}$$

We also have, from the Bernoulli equation,

$$C_p = 1 - \frac{U^2}{U_\infty^2} \tag{2.4}$$

or, expressing U in the form

$$U = \Gamma(x) \cos \alpha(x) \tag{2.5}$$

where U is the tangential velocity and α the angle of the tangent with the x-axis at a point on the body, and putting $r^2 = f(x)$, we obtain

$$U = \Gamma(x) \left[4f/(4f+f'^2)\right]^{1/2} \tag{2.6}$$

Using (2.6) and (2.4), (2.3) may be written as

$$C_D = - \frac{16}{U_\infty^2 d^2} \int_0^L \Gamma^2(x) \left[ff'/(4f + f'^2)\right] dx \tag{2.7}$$

The above equation, which is valid for axisymmetric, irrotational flow about a body of revolution immersed in a uniform stream, should give the value zero.

We shall now derive a form of C_D when an axial downstream sink of strength M is present. Since the boundary condition and the Laplace equation are homogeneous and linear superposition of solutions is valid, $\Gamma(x)$ may be assumed to be of the form

$$\Gamma(x) = U_\infty \Gamma_1 + M\Gamma_2 \tag{2.8}$$

Here Γ_1 is nondimensional, but Γ_2 has the dimensions L^{-2}. Substituting for $\Gamma(x)$ in (2.7) and noting that, with the uniform stream alone, the drag is zero, we now obtain

$$C_D = \frac{-16}{U_\infty^2 d^2} \int_0^L (2MU_\infty \Gamma_1 \Gamma_2 + M^2 \Gamma_2^2)[ff'/(4f+f'^2)]dx \tag{2.9}$$

Hence the drag coefficient C_D can be written as

$$C_D = AM' + BM'^2 \tag{2.10}$$

where $M' = \frac{M}{U_\infty d^2}$ and A and B are the nondimensional coefficients

$$\begin{aligned} A &= -32 \int_0^L \Gamma_1 \Gamma_2 [ff'/(4f+f'^2)]dx \\ B &= -16\, d^2 \int_0^L \Gamma_2^2 [ff'/(4f+f'^2)]dx \end{aligned} \tag{2.11}$$

The coefficients A and B of (2.9) were calculated from (2.11) by determining Γ_1 and Γ_2 from the aforementioned program of Landweber and Choi. The results obtained are

$A = - 0.98195474$

$B = 0.79076785$

Thus C_D is given by a quadratic equation in M', (2.10).

The approximate drag coefficient of a low drag body at a Reynolds number of the order of 10^6, is about 0.04. We also know that the viscous pressure drag is approximately 0.1 times that of the total drag and is also approximately equal to the thrust deduction. Hence a drag coefficient C_D of 0.004 was used in the present calculations. Solving the quadratic equation for M'we obtain the value of M' = -0.004 for the sink; the other value for M'is neglected since it is positive.

CHAPTER III

IRROTATIONAL FLOW

The irrotational flow outside the boundary layer and wake can be derived as a solution of an exterior Neumann problem of potential theory. As is well known, this type of problem can be solved by setting up an integral equation of the second kind in a surface distribution of singularities. In the present problem, an integral equation of the first kind is considered, for three reasons. Firstly, the calculation is relatively simple and less time-consuming in comparison with methods based on an integral equation of the second kind. Secondly, the boundary conditions can be prescribed in the form of the stream function on the 'fixed matching boundary' and the solution of the integral equation yields directly the velocity distribution on the boundary which is required as an input for the boundary-layer and wake calculation. This avoids additional operations, such as numerical integration or differentiation, on the solution of the integral equation for the subsequent boundary-layer calculation to obtain the necessary boundary conditions for the potential-flow calculations. Thirdly, the high accuracy given by the integral equation of the second kind is not required for boundary-layer calculations.

For the present case, with a sink on the axis behind the tail, the integral equation has to be rederived. For this purpose let us consider the general case of a body introduced into a flow field of undisturbed velocity potential ϕ_o.

1. Irrotational Flow Outside the Closed Body

See (Fig. 3.1) The total velocity potential Φ can be written as

$$\Phi = \phi_o + \phi \tag{3.1}$$

where, ϕ_o denotes the velocity potential of the ambient flow field and ϕ the disturbance potential due to the introduction of the body. The boundary condition on the surface S of the body is

$$\frac{\partial \Phi}{\partial n} = \frac{\partial \phi_o}{\partial n} + \frac{\partial \phi}{\partial n} = 0 \tag{3.2}$$

where n denotes the distance normal to S from a point on S. Let $\phi_d = -(x-t)/R^3$, $\psi_d = r^2/R^3$ denote the potential and stream functions of a doublet of unit strength oriented in the positive x-direction at a point (t,0) on the axis, and

$$R = [(x-t)^2 + r^2(x)]^{1/2} \tag{3.3}$$

The equation of the body is $r^2 = f(x)$, $0 \leq x \leq L$ in cylindrical coordinates (x,r). Let U (x) be the tangential velocity at a point on the body surface, s the arc length measured from the nose N of the body, and ℓ the length of arc from the nose to the tail along a meridian. By Green's reciprocal theorem, we have

$$\int_S \phi \frac{\partial \phi_d}{\partial n} \, dS = \int_S \phi_d \frac{\partial \phi}{\partial n} \, dS \tag{3.4}$$

where dS is the surface area element. By (3.2) and (3.4) we have

$$\int_0^{\ell} r\phi \frac{\partial \phi_d}{\partial n} \, ds = - \int_0^{\ell} r \, \phi_d \frac{\partial \phi_o}{\partial n} \, ds \tag{3.5}$$

where ds is the element of arc length. Since

$$r \frac{\partial \phi_d}{\partial n} = - \frac{\partial \psi_d}{\partial s}, \quad r \frac{\partial \phi_o}{\partial n} = - \frac{\partial \psi_o}{\partial s} \tag{3.6}$$

where ψ_o denotes the stream function corresponding to ϕ_o, (3.5) then becomes

$$\int_0^{\ell} \phi \frac{\partial \psi_d}{\partial s} \, ds = - \int_0^{\ell} \phi_d \frac{\partial \psi_o}{\partial s} \, ds$$

By integration by parts, we obtain

$$\phi\psi_d \Big|_0^{\ell} - \int_0^{\ell} \psi_d \frac{\partial \phi}{\partial s} \, ds = - \int_0^{\ell} \phi_d \frac{\partial \psi_o}{\partial s} \, ds$$

Since $r = 0$ at $s = 0$ and $s = \ell$, $\psi_d = 0$ at both ends, and, by substituting $\frac{\partial \phi}{\partial s} = \frac{\partial \Phi}{\partial s} - \frac{\partial \phi_o}{\partial s} = U - \frac{\partial \phi_o}{\partial s}$, we obtain

$$\int_0^{\ell} U \frac{r^2(x)}{R^3} \, ds = \int_0^{\ell} \left[\psi_d \frac{\partial \phi_o}{\partial s} + \phi_d \frac{\partial \psi_o}{\partial s}\right] ds \tag{3.7}$$

Equation (3.7) is in the form of an integral equation of the first kind for U_s since the right member is a known function.

It can, however, be shown that $[\psi_d \, d\phi_o + \phi_d \, d\psi_o]$ is an exact differential (see Appendix). Consequently the integral of the right hand side of equation (3.7) is independent of the path of integration between nose and tail points of the body. Hence the integral may be evaluated along the indicated path in Fig. 3.2, along the axis from nose N to the tail T, with the doublet at (t,0) avoided by means of a semi-circle of very small radius R.

Along the axis, we have $\psi_d = 0$, and since ψ_o is an axisymmetric stream function, $\psi_o(x,0)$ is a constant along the axis. Hence, we need to evaluate the right member of (3.7) only along the small semicircle. Then the integral becomes

$$\int_o^{\ell} [\psi_d \frac{\partial \phi_o}{\partial s} + \phi_d \frac{\partial \psi_o}{\partial s}] \, ds = - \int_o^{\pi} [\frac{\sin^2\theta}{R} \frac{\partial \phi_o}{\partial \theta} - \frac{\cos\theta}{R^2} \frac{\partial \psi_o}{\partial \theta}] \, d\theta$$

where use has been made of the relations $r = R \sin\theta$; $x - t = R \cos\theta$ and R is very small. We have for $\frac{\partial \phi_o}{\partial \theta}$ and $\frac{\partial \psi_o}{\partial \theta}$,

$$\begin{aligned} \frac{\partial \phi_o}{\partial \theta} &= - R \sin\theta \frac{\partial \phi_o}{\partial x} + R \cos\theta \frac{\partial \phi_o}{\partial r} \\ \frac{\partial \psi_o}{\partial \theta} &= - R \sin\theta \frac{\partial \psi_o}{\partial x} + R \cos\theta \frac{\partial \psi_o}{\partial r} \\ &= R \sin\theta \; r \frac{\partial \phi_o}{\partial r} + R \cos\theta \; r \frac{\partial \phi_o}{\partial x} \end{aligned} \qquad (3.8)$$

We now expand $(\frac{\partial \phi_o}{\partial x})_{(x,r)}$ and $(\frac{\partial \phi_o}{\partial r})_{(x,r)}$ in Taylor series about the point (t,o):

$$\left(\frac{\partial \phi_o}{\partial x}\right)_{(x,r)} = \left(\frac{\partial \phi_o}{\partial x}\right)_{t,0} + (x-t)\left(\frac{\partial^2 \phi_o}{\partial x^2}\right)_{t,0} + r\left(\frac{\partial^2 \phi_o}{\partial x \partial r}\right)_{t,0} + \cdots$$

$$\left(\frac{\partial \phi_o}{\partial r}\right)_{(x,r)} = \left(\frac{\partial \phi_o}{\partial r}\right)_{t,0} + (x-t)\left(\frac{\partial^2 \phi_o}{\partial x \partial r}\right)_{t,0} + r\left(\frac{\partial^2 \phi_o}{\partial r^2}\right)_{t,0} + \cdots \qquad (3.9)$$

Using the fact that $\left(\frac{\partial \phi_o}{\partial r}\right) = 0$ by symmetry in (3.9) and neglecting higher order terms, we obtain from (3.8)

$$\frac{\partial \phi_o}{\partial \theta} = -R \sin\theta \left(\frac{\partial \phi_o}{\partial x}\right)_{t,0}$$

$$\frac{\partial \psi_o}{\partial \theta} = R^2 \sin\theta \cos\theta \left(\frac{\partial \phi_o}{\partial x}\right)_{t,0} \qquad (3.10)$$

Hence the integral becomes

$$\int_o^{\ell} U_s \frac{r^2}{R^3}\, ds = 2\left(\frac{\partial \phi_o}{\partial x}\right)_{t,0} \qquad (3.11)$$

If $\phi_o = U_\infty x$ where $U_\infty = 1$, equation (3.11) reduces to the well-known integral equation for U_s on the surface of an axisymmetric body placed in a uniform stream of unit velocity,

$$\int_o^{\ell} U_s \frac{r^2}{R^3}\, ds = 2$$

2. Irrotational Flow Past the Semi-Infinite Body Enclosing the Boundary Layer and Wake

S_F is a fixed matching boundary, (FMB) enclosing the boundary layer and wake, s is the arc length along a meridian measured from the nose N, n is the distance normal to S_F from a point on S_F and Ψ the value of the stream

function corresponding to the total velocity potential Φ, is prescribed along s. See fig. [3.3]. The boundary condition on the surface S_F is given by

$$\frac{\partial \Phi}{\partial n} = \frac{\partial \phi_o}{\partial n} + \frac{\partial \phi}{\partial n}$$

or (3.12)

$$\frac{\partial \Psi}{\partial s} = \frac{\partial \psi_o}{\partial s} + \frac{\partial \psi}{\partial s}$$

Applying Green's reciprocal theorem to potentials ϕ_d and ϕ gives

$$\int_{S_F} \phi \frac{\partial \phi_d}{\partial n} dS = \int_{S_F} \phi_d \frac{\partial \phi}{\partial n} dS \tag{3.13}$$

where dS is the surface area element. From (3.12) and (3.13) we obtain

$$\int_o^\infty r \phi \frac{\partial \phi_d}{\partial n} ds = \int_o^\infty r \phi_d [\frac{\partial \Phi}{\partial n} - \frac{\partial \phi_o}{\partial n}] ds \tag{3.14}$$

Using (3.6) and the relation $r \frac{\partial \Phi}{\partial n} = -\frac{\partial \Psi}{\partial s}$ in (3.14), we find

$$\int_o^\infty \phi \frac{\partial \psi_d}{\partial s} ds = \int_o^\infty \phi_d \frac{\partial \Psi}{\partial s} ds - \int_o^\infty \phi_d \frac{\partial \psi_o}{\partial s} ds$$

or, after integration by parts, the above equation may be written as

$$\int_o^\infty \frac{\partial \phi}{\partial s} \psi_d ds = \phi \psi_d \Big|_o^\infty - \int_o^\infty \phi_d \frac{\partial \Psi}{\partial s} ds + \int_o^\infty \phi_d \frac{\partial \psi_o}{\partial s} ds$$

Since $\frac{\partial \phi}{\partial s} = \frac{\partial \Phi}{\partial s} - \frac{\partial \phi_o}{\partial s} = U - \frac{\partial \phi_o}{\partial s}$, $r = 0$ at $s = 0$, and $\phi\psi_d$ as $R \to \infty$ is zero this becomes

$$\int_o^\infty U \frac{r^2}{R^3} ds = - \int_o^\infty \phi_d \frac{\partial \Psi}{\partial s} ds + \int_o^\infty [\psi_d \frac{\partial \phi_o}{\partial s} + \phi_d \frac{\partial \psi_o}{\partial s}] ds \qquad (3.15)$$

The integral $\int [\phi_d \frac{\partial \psi_o}{\partial s} + \psi_d \frac{\partial \phi_o}{\partial s}] ds$ is independent of the path of integration and, as was shown in the previous section, is equal to $2(\frac{\partial \phi_o}{\partial x})_{t,0}$. Hence, we obtain

$$\int_o^\infty U \frac{r^2}{R^3} ds = \int_o^\infty \phi_d \frac{\partial \Psi}{\partial s} ds + 2(\frac{\partial \phi_o}{\partial x})_{t,0}$$

or (3.16)

$$\int_o^\infty U \frac{r^2}{R^3} ds = \int_o^\infty \Psi \frac{\partial \phi_d}{\partial s} ds + 2(\frac{\partial \phi_o}{\partial x})_{t,0}$$

Since $\Psi(0) = 0$ and $\phi_d \Psi \to 0$ as $R \to \infty$.

3. Velocity at Matching Boundary in Presence of an External Sink

The interaction of the boundary layer and wake with irrotational flow is solved by an iteration procedure [3]. It is now necessary to take into account the effect of an external sink on these calculations, since a sink is chosen for the present "thrust deduction" calculation (Ch. II). The normal velocity to the FMB and the value of the stream function on the FMB due to an external sink and its image system within the body are required. The normal velocity and stream functions at the FMB, calculated by the interaction procedure for the flow without the external sink, will now be modified by the contributions of the sink

and its associated disturbance potential in the potential flow. These updated values of normal velocity and stream function on the FMB are used to calculate the external potential flow (outside BLW) once more, and the resulting pressure distribution is used to calculate the BLW.

a) Method 1: Using Green's third formula. The tangential velocity U on the surface of the body is obtained by solving a Fredholm integral equation of first kind, in the presence of an external axial sink. The disturbance velocity potential on the surface of the body can then be written as

$$\phi_Q(x,r_b) = \int_0^S U\, ds - \frac{M}{R_s} \tag{3.17}$$

where here, and in the following, $Q(\xi,\eta,\zeta)$ denotes a point on the body surface, M the sink strength, $R_s = [(\xi-x_s)^2 + \eta^2 + \zeta^2]^{1/2}$ is the distance from the position $S(x_s,0)$ of the sink to a point Q on the body.

With this value of the disturbance potential on the surface, Green's third formula can be used to calculate the disturbance potential ϕ_p at any point P(x,y,0) in the field. We have, by Green's third formula,

$$\phi_p = \frac{1}{4\pi} \int_S \left[\phi_Q \frac{\partial}{\partial n_Q}\frac{1}{R_{PQ}} - \frac{1}{R_{PQ}}\frac{\partial \phi_Q}{\partial_{nQ}}\right] dS_Q \tag{3.18}$$

where $R_{PQ} = [(x-\xi)^2 + (y-\eta)^2 + \zeta^2]^{1/2}$ is the distance between the points P and Q. [See fig (3.4)].

The boundary condition on the body surface is that the normal velocity is zero,

$$\frac{\partial \phi_Q}{\partial n_Q} + \frac{\partial \phi_s}{\partial n_Q} = 0 \text{ on } S,\ \phi_s = \frac{M}{R_s}$$

or

$$\frac{\partial \phi_Q}{\partial n_Q} = - M \frac{\partial}{\partial n_Q} \frac{1}{R_s} \tag{3.19}$$

We have

$$\frac{\partial}{\partial n_Q} \frac{1}{R_s} = \frac{-1}{R_s^3} [-(x_s-\xi)\ell_Q + \eta m_Q + \zeta n_Q]$$

and

$$\frac{\partial}{\partial n_Q} \frac{1}{R_{PQ}} = \frac{1}{R_{PQ}^3} [(x-\xi)\ell_Q + (y-\eta)m_Q - \zeta n_Q]$$

where ℓ_Q, m_Q and n_Q are the direction cosines of the normal to the body at the point Q and are given by

$$\ell_Q = - \frac{f'(\xi)}{D_Q}, \quad m_Q = \frac{2\eta}{D_Q}, \quad n_Q = \frac{2\zeta}{D_Q} \quad \text{and} \quad D_Q = \sqrt{f'^2 + 4f}$$

With the help of relations for ℓ, m, n and noting that $\eta = r_Q \cos \theta_Q$ $\zeta = r_Q \sin \theta_Q$ and $y = r_p$ when $\theta_p = 0$ in cylindrical coordinates, we can rewrite the above equations as,

$$\frac{\partial}{\partial n_Q} \frac{1}{R_s} = - \frac{1}{D_Q R_s^3} [(x_s - \xi)f' + 2r_Q^2] \tag{3.20}$$

and

$$\frac{\partial}{\partial n_Q} \frac{1}{R_{PQ}} = - \frac{1}{D_Q R_{PQ}^3} [(x - \xi)f' - 2r_p r_Q \cos \theta_Q + 2r_Q^2] \tag{3.21}$$

Consider a source situated at the point P. Then by Gauss flux theorem, we have

$$\int_S \frac{\partial}{\partial n_Q} \frac{1}{R_{PQ}} \, dS_Q = 0 \tag{3.22}$$

Equation (3.22) is used to remove the peak in the integral of equation (3.18) by writing it in the form

$$\phi_P = \frac{1}{4\pi} \int_S \left[(\phi_Q - \phi_{P'}) \frac{\partial}{\partial n_Q} \frac{1}{R_{PQ}} - \frac{1}{R_{PQ}} \frac{\partial \phi_Q}{\partial n_Q} \right] ds_Q \tag{3.23}$$

where $\phi_{P'}$ is the potential at the point P', the point on the body such that PP' is normal to the body. When R_{PQ} is small, $(\phi_Q - \phi_{P'})$ is also small.

Equation (3.23) may be written as

$$\phi_P = \frac{1}{4\pi} \int_o^p \left\{ (\phi_Q - \phi_{P'}) \int_0^{2\pi} \frac{\partial}{\partial n_Q} \frac{1}{R_{PQ}} \, d\theta_Q - \frac{\partial \phi_Q}{\partial n_Q} \int_0^{2\pi} \frac{1}{R_{PQ}} \, d\theta_Q \right\} ds \tag{3.24}$$

where p is the distance from nose to tail measured along a meridian and ds is an element of arc length. We have, from equation (3.21),

$$\int_0^{2\pi} \frac{\partial}{\partial n_Q} \frac{1}{R_{PQ}} \, d\theta = - \frac{1}{D_Q} \left[(x-\xi) f' + 2 r_Q^2 \right] \int_0^{2\pi} \frac{1}{R_{PQ}^3} \, d\theta + \frac{2 r_Q r_P}{D_Q} \int_0^{2\pi} \frac{\cos\theta}{R_{PQ}^3} \, d\theta \tag{3.25}$$

We now need to evaluate the integrals

$$I_1 = \int_0^{2\pi} \frac{1}{R_{PQ}^3} \, d\theta, \quad I_2 = \int_0^{2\pi} \frac{\cos\theta}{R_{PQ}^3} \, d\theta, \quad I_3 = \int_0^{2\pi} \frac{d\theta}{R_{PQ}}$$

We can write

$$R_{PQ}^2 = (x-\xi)^2 + r_P^2 + r_Q^2 - 2r_P r_Q \cos\theta_Q$$

$$= (x-\xi)^2 + (r_P+r_Q)^2 - 4r_P r_Q \cos^2 \theta/2$$

$$= R'^2 \left[1-k^2 \cos^2 \frac{\theta_Q}{2}\right]$$

where

$$R'^2 = (x-\xi)^2 + (r_P+r_Q)^2,\ k^2 = 4r_P r_Q/R'^2$$

Substituting $\beta = \frac{1}{2}(\pi-\theta)$ in the above integrals, we obtain

$$I_1 = \int_0^{2\pi} \frac{1}{R_{PQ}^3} d\theta = \frac{4}{R'^3} \int_0^{\pi/2} \frac{d\beta}{[1-k^2\sin^2\beta]^{3/2}} = \frac{4}{R'^3} \frac{E(k)}{1-k^2}$$

$$I_2 = \int_0^{2\pi} \frac{\cos\theta}{R_{PQ}^3} d\theta = -\frac{4}{R'^3} \int_0^{\pi/2} \frac{1-2\sin^2\beta}{[1-k^2\sin\beta]^{3/2}} d\beta$$

$$= \frac{4}{R'^3} \frac{2-k^2}{k^2} \cdot \frac{E(k)}{1-k^2} = \frac{8}{R'^3 k^2} K(k)$$

$$I_3 = \int_0^{2\pi} \frac{1}{R_{PQ}} d\theta = \frac{4}{R'} \int_0^{\pi/2} \frac{1}{[1-k^2\sin^2\beta]^{1/2}} d\beta$$

$$= \frac{4}{R'} K(k)$$

where K(k) and E(k) are the elliptic integrals of first and second kind respectively. We have

$$1-k^2 = 1 - \frac{4r_P r_Q}{(x-\xi)^2 + (r_P+r_Q)^2} = \frac{R_{PQ}'^2}{R'^2} \tag{3.26}$$

where

$$R_{PQ}'^2 = (x-\xi)^2 + (r_P-r_Q)^2 \text{ and}$$

$$\frac{2-k^2}{k^2(1-k^2)} = \frac{1}{1-k^2} + \frac{2}{k^2} = \frac{R'^2}{R_{PQ}'^2} + \frac{R'^2}{2r_P r_Q} \tag{3.27}$$

Substituting (3.26) and (3.27) in I_1, I_2, and I_3 and rewriting (3.24) with the help of I_1, I_2, I_3 and (3.21), we obtain, after collecting terms,

$$\phi_P = \frac{1}{\pi} \int_0^P \left\{ \left[\frac{(\phi_Q - \phi_{P'})}{R'} \right] \left\{ (E-k) + \frac{E}{R_{PQ}^2} [2r_Q(r_P - r_Q) - (x-\xi) f'(\xi)] \right\} - \frac{M}{R_s^3} [(x_s - \xi) f' + 2r_Q^2] \frac{K(k)}{R'} \right\} \frac{r_Q}{D_Q} \, d\xi \tag{3.28}$$

We have $ds = dx \sec \alpha = \frac{D_Q}{2r_Q}$, where α is the angle made by the tangent with the x-axis. ϕ_P can now be written as

$$\phi_P = \frac{1}{2\pi} \int_{-1}^{1} \left\{ \frac{(\phi_Q - \phi_{P'})}{R'} \cdot (E-K) + \frac{\phi_Q - \phi_{P'}}{R'} \cdot \frac{E}{R_{PQ}^2} [2r_Q(r_P - r_Q) - (x-\xi) f(\xi)] - \frac{M}{R_s^3} \frac{K}{R'} [(x_s - \xi) f' + 2r_Q^2) \right\} dx \tag{3.29}$$

where the body extends between x = -1 and 1.

Equation (3.29) is used to calculate the disturbance potential at five closely-spaced points, two on either side of the fixed point where the normal velocity to FMB is desired, and one coinciding with the fixed point. The five points are taken along the normal to FMB at this point. The normal derivative of the potential is obtained by fitting a Lagrange interpolation polynomial through these five points. The normal derivative of the disturbance potential yields the normal disturbance velocity $\bar{V} \cdot \bar{n}$. To obtain the total normal velocity, that due to the sink is to be added to the above value of $\bar{V} \cdot \bar{n}$.

The velocity at a point P due to a sink of strength M placed at a point $(x_s, 0, 0)$ is given by

$\bar{V}_s = \frac{M}{R_s^3} \cdot \bar{R}_s$ where $\bar{R}_S = (x_s - x_1)\bar{i} - r_1\bar{j}$ is the position vector of $(x_s, 0)$ with respect to $P(x_1, r_1, 0)$. The normal velocity at the point P due to the sink alone is given by

$$\bar{V}_s \cdot \bar{n} = \frac{M}{R_s^3} (\bar{R}_s \cdot \bar{n})$$

$$= \frac{M}{R_s^3} [(x_s - x_1)\ell_1 - r_1\ell_2] \qquad (3.30)$$

where ℓ_1 and ℓ_2 are direction cosines of the normal at FMB.
The net normal velocity V at P due to the sink and its image system can be written as

$$V = \bar{V} \cdot \bar{n} + \bar{V}_s \cdot \bar{n} \qquad (3.31)$$

Having calculated the normal velocity V the stream function ψ at any point can be calculated by integrating V along a meridian from the nose

$$\psi = -\int_0^s r\, V \, ds \qquad (3.32)$$

The tangential velocity U on the body surface, used as an input to Green's third formula in calculating the velocity potentials and hence the normal velocities at the FMB, is obtained by solving an integral equation of first kind in U. This velocity is accurate upto four significant digits only. Due to the nature of integral equations of the first kind, greater accuracy cannot be expected from this solution. When this

solution was used in Green's third formula to calculate velocity potential, it failed to give a good estimate of the normal velocity at FMB. This is so because the calculation of normal velocity involves differences in velocity potentials of nearly equal magnitudes. This became apparent when the computer program was checked with the exact solution for a sphere. The use of Green's third formula demands inputs that are more accurate than that given by the solution of an integral equation of the first kind. As a result, it was decided to try a different approach to obtain both normal and tangential velocities due to the sink and its image systems at FMB, as presented in the next section.

b) Method 2: Using Taylor series. By this method, we can not only estimate the normal velocity at FMB due to the sink and its image system, but we can also estimate the tengential velocity at FMB due to the sink and its image system. This eliminates the need to solve an integral equation for flow past the semi-infinite body including the effect of the sink. Instead, the calculated normal and tangential velocities due to the sink and its image system within the body are added vectorially to those obtained by solving an integral equation (3.16) for uniform flow past the semi-infinite body.

The resulting pressure distribution is used to calculate the turbulent boundary-layer once more, thus incorporating the effect of the sink on the calculation procedure.

Equation (3.11) was solved to obtain the surface distribution of tangential velocity u(s,0) on the closed body. Since the FMB is not very far from the body, it is assumed that the normal to the body is also normal to the FMB. Now a procedure for estimating normal and tangential

velocities at FMB due to the sink and its image system will be presented. By Taylor series, we can write for U and V

$$U(s,n) = U(s,0) + n\, U_s(s,0) + \frac{n^2}{2} U_{ss}(s,0) + \ldots\ldots \tag{3.33}$$

$$V(s,n) = V(s,0) + n\, V_s(s,0) + \frac{n^2}{2} V_{ss}(s,0) + \ldots \tag{3.34}$$

By noting that the normal velocity on the body surface is zero and neglecting higher-order terms, we can write

$$U(s,n) \simeq U(s,0) + n\, U_s(s,0) + \frac{n^2}{2} U_{ss}(s,0) \tag{3.35}$$

$$V(s,n) \simeq n\, V_s(s,0) + \frac{n^2}{2} V_{ss}(s,0) \tag{3.36}$$

We have the equation of continuity

$$\frac{\partial}{\partial s}(rU) + \frac{\partial}{\partial n}(h_1 rV) = 0 \tag{3.37}$$

Since the flow is irrotational, we have

$$\frac{\partial V}{\partial s} - \frac{\partial}{\partial n}(h_1 U) = 0 \tag{3.38}$$

where $r = r_b(s) + n \cos r(s)$, $h_1 = 1 + nK(s)$ is the longitudinal metric coefficient, $K(s)$, $\alpha(s)$ and $r_b(s)$ are the longitudinal curvature of the body, the angle of the tangent to the body with the x-axis and the body ordinate at the point $(s,0)$ on the body, respectively. In the following equations, the notation $U(s,n)$, $V(s,n)$ etc., has been omitted and U,V, etc., will be used for simplicity. Eqns. (3.37) and (3.38) may be written as

$$rU_s + Uh_1 \sin\alpha + h_1 r\, V_n + V[rK + h_1 \cos\alpha] = 0 \tag{3.39}$$

and

$$V_s - U_n - Uk = 0 \tag{3.40}$$

where α is the angle made by the tangent with the x-axis. Differentiating (3.39) with respect to n and s we have, respectively

$$\begin{aligned} rU_{ss} &+ 2U_s h_1 \sin\alpha + U(K'n \sin\alpha - Kh_1 \cos\alpha) + h_1 r\, V_{sn} \\ &+ V_n(K'nr + h_1^2 \sin\alpha) + V_s(rK + h_1 \cos\alpha) \\ &+ V(Kh_1 \sin\alpha + rK' + K'n \cos\alpha - h_1 K \sin\alpha) = 0 \end{aligned} \tag{3.41}$$

and

$$\begin{aligned} rU_{sn} &+ U_s \cos\alpha + U_n h_1 \sin\alpha + kU \sin\alpha + h_1 r\, V_{nn} \\ &+ 2V_n(rK + h_1 \cos\alpha) + 2KV \cos\alpha = 0 \end{aligned} \tag{3.42}$$

Similarly we have from (3.40)

$$V_{ss} - U_{sn} - KU_s - K'U = 0 \tag{3.43}$$

and

$$V_{sn} - U_{nn} - KU_n = 0 \tag{3.44}$$

In deriving the above equations, the relations

$\frac{dr}{ds} = -K$ and $\frac{dK}{ds} = K'$ and $\frac{\partial r}{\partial s} = h_1 \sin\alpha$ have been used.

Putting n = 0 in the equations (3.39) to (3.44) and using the subscript 0 to denote the values at n = 0, and also observing that $V_o = V_{s0} = V_{ss0} = 0$, we obtain

$$r_b U_{s0} + U_o \sin\alpha + r_b V_{no} = 0 \tag{3.45}$$

$$U_{n0} + U_0 K = 0 \tag{3.46}$$

$$r_b U_{ss0} + r_b V_{sn0} + 2U_{s0} \sin\alpha = 0 \tag{3.47}$$

$$r_b U_{sn0} + U_{s0} \cos\alpha + U_{n0} \sin\alpha + KU_o \sin\alpha + r_b V_{nn0} + 2V_{n0} (Kr_0 + \cos\alpha) = 0 \tag{3.48}$$

$$V_{sn0} + KU_{s0} + K'U_0 = 0 \tag{3.49}$$

$$V_{sn0} - U_{nn0} - K U_{n0} = 0 \tag{3.50}$$

By (3.45), we have

$$V_n(s,0) = V_{n0} = - U_0 \frac{\sin\alpha}{r_b} - U_{s0} \tag{3.51}$$

From (3.46),

$$U_n(s,0) = U_{n0} = - U_o K \tag{3.52}$$

From equations (3.48), (3.45), (3.46) and (3.49), we obtain

$$V_{nn}(s,0) = V_{nn0} = U_s(s,0) \left[3K + \frac{\cos\alpha}{r_b}\right] + U(s,0)\left[K' + \frac{2K\sin\alpha}{r_b} + \frac{2\sin\alpha\cos\alpha}{r_b^2}\right] \tag{3.53}$$

From (3.50), (3.49), (3.46) and (3.45), we have

$$U_{nn}(s,0) = U_{nn0} = -U_{ss}(s,0) - U_s(s,0) \frac{\sin\alpha}{r_b} + \frac{U(s,0)}{r_b^2}[K^2 r_b^2 + Kr_b \sin\alpha + \sin^2\alpha] \tag{3.54}$$

In the above equations, $U(s,0)$ is the solution of the integral equation (3.11), and hence $U_s(s,0)$ and $U_{ss}(s,0)$ are calculated numerically. Having thus obtained V_n, U_n, V_{nn} and U_{nn} from equations (3.51) through (3.54), we can now calculate $U(s,n)$ and $V(s,n)$ from equations (3.35) and (3.36).

CHAPTER IV

THICK BOUNDARY LAYER AND NEAR WAKE

This chapter describes the method of calculating the development of the thick turbulent boundary layer over the body and wake. The complete Reynolds equations for the mean flow were first examined, and suitable approximations were made to simplify them in [4]. The resulting equations are elliptic and contain a number of additional terms in comparison with the usual thin boundary-layer equations.

1. Governing Equations

The momentum and continuity equations for a thick, axisymmetric boundary layer, given in [5], are

$$\frac{U}{h_1}\frac{\partial U}{\partial x} + V\frac{\partial U}{\partial y} + \frac{K}{h_1}UV + \frac{1}{\rho h_1}\frac{\partial p}{\partial x} = \frac{1}{r h_1}\frac{\partial}{\partial y}\left(\frac{h_1 r\tau}{\rho}\right) \tag{4.1}$$

$$\frac{U}{h_1}\frac{\partial V}{\partial x} + V\frac{\partial V}{\partial y} - \frac{K}{h_1}U^2 + \frac{1}{\rho}\frac{\partial p}{\partial y} = 0 \tag{4.2}$$

$$\frac{\partial}{\partial x}(Ur) + \frac{\partial}{\partial y}(rh_1 V) = 0 \tag{4.3}$$

where U and V are the mean velocity components in the boundary layer along tangential and normal directions of the body, p is the pressure at a point, $h_1 = 1 + Ky$, is the metric coefficient in the longitudinal direction, $\tau = -\rho\,\overline{uv} + \mu\frac{\partial U}{\partial y}$ is the shear stress and μ is the dynamic viscosity of the fluid. See fig [4.1].

Equation (4.2), in which viscous and turbulence terms are neglected, implies that the viscous and turbulent stresses acting in the normal direction are negligible in comparison with the pressures and the variation of static pressure across the boundary layer is associated primarily with the curvature of the mean-flow streamlines.

2. Turbulence Model

The adopted turbulence model discussed in [3] is written here for convenience. The equation for the conservation of turbulent kinetic energy was transformed into one for the Reynolds stress τ:

$$\frac{1}{2a_1}\left(\frac{U}{h_1}\frac{\partial\tau}{\partial x} + V\frac{\partial\tau}{\partial y}\right) - \tau\left(\frac{\partial U}{\partial y} - KU\right) + \frac{1}{r}\frac{\partial}{\partial y}\left[\left(rG\frac{\tau}{a_1^{3/2}}\sqrt{\frac{\tau_{max}}{\rho}}\right)\right] + \frac{1}{\ell}\frac{\tau^{3/2}}{\rho^{1/2}} = 0 \qquad (4.4)$$

where a_1 $\left(= -\frac{\overline{uv}}{q^2}\right)$ is a constant (=0.15), $G(y/\delta)$ is a diffusion function and $\ell(y/\delta)$ is a length-scale function identified with the usual mixing length.

The equation for 'ℓ' that was used is given by

$$\frac{\ell}{\ell_o} = 1 + \frac{\alpha e_{eff}}{\left(\frac{\partial U}{\partial y}\right)} \qquad (4.5)$$

and

$$\frac{d}{dx}(e_{eff}) = (e - e_{eff})/(10\delta)$$

where ℓ_o is the length scale with the usual rate of strain $\frac{\partial U}{\partial y}$. ℓ is the length scale with the extra rate of strain e and α is a constant of the order 10, e_{eff} is the effective rate of strain, 10δ represents the lag length over which the boundary layer responds to a change in e.

3. Method of Solution

The axisymmetric laminar boundary layer from the nose to the natural point of transition was calculated by using Thwaite's method. From the natural point of transition onward, equations (4.1), (4.2) and (4.3) were used to calculate the thick turbulent boundary layer.

Equations (4.1), (4.2) and (4.3) contain four unknowns, namely U,V,p and $\overline{uv}$. Even when a turbulent model is introduced for $\overline{uv}$, the resulting set of equations cannot be solved by a marching technique. This is due to the presence of the pressure as an unknown.

Equations (4.1) and (4.3) are first solved by a marching technique for U and V for an assumed pressure field p(x,y). The y momentum equation (4.2) is then used to update the pressure field. In this iteration scheme, the solution for the pressure p and of the y momentum equation lags the velocity field by one iteration. The solution is obtained through step-by-step integration by marching downstream from some initial station where the velocity and shear-stress profiles are prescribed. In the wake calculation, the conditions $\tau = 0$ and $\frac{\partial U}{\partial y} = 0$ at the wake centerline are used.

CHAPTER V

INTERACTION-ITERATION PROCEDURE

To begin with, the velocity distribution on the body is calculated from the integral equation of the first kind for the unknown velocity for irrotational flow outside the body. Using the above-calculated pressure distribution, the laminar boundary layer is calculated up to the natural point of transition, and, from then onwards, the turbulent boundary layer is calculated. In continuing the calculations into the wake, the conditions $\frac{\partial U}{\partial y} = 0$ and $\tau = 0$ are applied on the wake centerline. The first time the boundary layer and wake are calculated, the matching boundary between the boundary layer and the external irrotational flow is fixed once and for all at 1.25δ from the wall. This ensures in this particular case that the fixed matching boundary always lies in the external irrotational flow. The stream function at the matching boundary is calculated and is used to calculate the normal velocity at the matching boundary. This, in turn, is used as a Neumann boundary condition for the external potential flow. This solution is then employed to update the pressures along the boundary, and the turbulent boundary layer is recalculated. This iteration procedure is carried out until the required convergence is achieved in the wall pressure distribution. Each time, the turbulent boundary layer is calculated from the point of natural transition, where velocity and shear stress profiles are given.

At this point it is important to note that, due to the coordinate transformation at the first station of the wake calculation, the results obtained in the wake are incorrect and so for the purposes of calculating the drag, a different control volume is used, as is described in Chapter VI, instead of the far-wake momentum thickness.

In the case of a sink behind the tail, the external irrotational flow equations were modified in Chapter III.

CHAPTER VI

CALCULATION OF DRAG

The purpose is to compare the computed values of the thrust deduction from potential flow and viscous flow methods. Since the drag experienced by a body in a uniform irrotational flow is zero, the calculated drag of the body with an external sink equals the difference in drags i.e. the "thrust deduction". The calculation of drag in potential flow will be discussed in Section 1. The difference in drags computed with and without a sink in viscous flow gives the value of the thrust deduction in viscous flow. This procedure will be described in Section 2.

1. Calculation of Drag in Potential Flow

As mentioned earlier [Ch. 1], a calculation procedure for drag in potential flow that is accurate by at least an order of magnitude higher than that given by the H.-S. method [2] is required. Such a method was derived and programmed by Landweber, L., and Choi, D.H., and will be presented here briefly.

An integral equation of the second kind in terms of the unknown vortex distribution (tangertial velocity) is solved.

Consider the case of the body stationary in a uniform stream of velocity u = 1 in the negative x-direction. Assume that the fluid within the body is at rest, and that the disturbance velocity field is generated by a vortex sheet of strength $\bar{\gamma}$ on the body surface.

Let u(s) denote the tangential velocity at the body surface and $\gamma(s)$ the magnitude of the vector $\bar{\gamma}$, where s is arc length along a meridian section, measured from the tail. See fig [6.1]. Then

$$u(s) = -\gamma(s) \tag{6.1}$$

The condition that the tangential velocity on the interior side of the body surface S be zero yields the integral equation

$$1/2\ \gamma(s) + \frac{1}{4\pi} \int_0^{\ell}\int_0^{2\pi} \frac{\bar{s}_p \cdot \bar{\gamma}_s x \bar{r}_{QP}}{r_{PQ}^3}\, r_t\, dt\, d\theta = \cos \alpha_s \tag{6.2}$$

in which the first term is contributed by the local vortex element, the second is that of the entire vortex sheet, given by the Biot-Savart law, and the third is due to the uniform stream. Here P denotes a fixed point at $(s,\theta_p = 0)$, and $Q(t,\theta)$ a variable point of integration in the arc length t and polar angle θ. The total length of arc along a meridian is ℓ. The notations $r_t = r(t)$, $r_s = r(s)$, $\bar{r}_{PQ}$ for the position vector of P relative to Q are used. The magnitude of $\bar{r}_{PQ}$ is given by

$$r_{PQ} = [(x_t - x_s)^2 + r_t^2 + r_s^2 - 2r_s r_t \cos\theta]^{1/2}$$

$$= [R_{st}^2 - 4\, r_s r_t \cos^2\theta/2]^{1/2}$$

where $R_{st}^2 = (x_t - x_s)^2 + (r_t + r_s)^2$

and α is the angle made by the tangent with the x axis.

The most evident problem faced in solving the integral equation is the numerical treatment of the singularity of the kernel. The product of the strength of the vortex sheet and the secant of the slope angle was chosen as an unknown variable instead of vortex distribution itself, since this product varies rather mildly over the entire body, whereas the secant of the slope angle, which appears in the resulting integral equation, goes to infinity at both ends of the body. Yet the integrand has a logarithmic singularity when the moving point and the fixed point coincide. This can be removed by adding an identity to the integral equation.

After evaluating the scalar triple product and putting $\Gamma(s) = \gamma(s) \sec \alpha_s$, eqn (6.2) becomes

$$\Gamma(s) = 2 - \frac{1}{4\pi} \int_0^{\ell} \int_0^{2\pi} \frac{\Gamma(t) r_t \cos\alpha_t}{r_s r_{PQ}^3} \{2r_s r_t - [f'(x_t - x_s) + 2f_s] \cos\theta\} \, d\theta dt \tag{6.3}$$

The above equation, after integrating with respect to θ and eliminating the singularity, has an integrand that remains finite at the body ends, and is of the form of a product of a slowly varying unknown function and a rapidly varying kernel, involving elliptic integrals.

To solve the above integral equation, the entire body is divided by a certain number of evenly spaced sections along the arc length at which the solution was sought. In order to achieve higher accuracy, however, it was necessary to subdivide each section further. At these

additional node points, the solution is not sought directly but obtained from the four-point Lagrange interpolation formula by taking advantage of the fact that the unknown is a slowly varying function. Now the integral equation is discretized with the use of a Simpson's rule and the resulting simultaneous equations are solved by the Gauss-Siedel interation procedure.

After the calculation of $\Gamma(s)$, C_D is calculated from the formula

$$C_D = -\frac{32}{d^2}\int_0^{\ell} \Gamma^2\left(\frac{f}{4f+f'}\right)^{3/2} f'ds \qquad (6.4)$$

where d is the maximum diameter and $r^2 = f(x)$ is the equation of the body.

At each stage, the method was applied to a spheroid of length-diameter ratio $\ell/d = 6.0$, and the resulting velocity distribution was compared with values from the known analytical solution. The pressure drag coefficient was computed for only half the spheroid for which an exact analytical formula is known. The computed value was $C_D = -0.00857572$; the exact value is -0.00857578 and this accuracy is considerably better than required for the thrust-deduction problem.

The above program was modified for an axial downstream sink in a uniform flow field and the drag on the body was computed for the EPH form with a non-dimensional sink strength of $M' = -0.004$ (Ch. 2). The computed drag coefficient is 0.00392.

2. Calculation of Viscous Drag

Due to the coordinate transformation at the first station of the wake calculation, the results obtained in the wake are not very accurate and so for the purposes of calculating the drag, a special control volume is used. This control volume is shown in fig [6.2]. The body is considered to be at the center of a circular channel of large radius, with the flow considered to be inviscid in the neighborhood of the channel wall. It is convenient to select as a boundary of the control surface a transverse section perpendicular to the x-axis, AB, far ahead of the body and a transverse ring made by CD, meeting another ring made by DE and enclosing the remaining tailpiece EF of the body.

E is the last point of calculation on the body surface and DE is the normal to the body meeting EBLW at the point D. In the boundary layer, the boundary of the control volume is chosen to be along the normal to the body because the boundary layer calculations are done in a tangential and normal coordinate system, and all the quantities are known along normals to the body.

The momentum theorem gives the expression for the drag D of a body in a steady flow,

$$D = - \int_S [p\ell + \rho u(\bar{V}\cdot\bar{n})]\, dS \qquad (6.5)$$

as an integral over a control surface S surrounding the body, where p is the pressure, $\bar{n}$ is the outwardly directed normal, ℓ, m and n are its direction cosines, $\bar{V}$ is the velocity vector, u_s the s

component of the velocity vector, u the x component of the velocity at points of the control surface and ρ the density of the fluid, assumed to be constant. Here the flow incident upon the body and the direction of the drag force are taken in the positive x-direction.

In applying the momentum equation (6.5) to the selected control volume, we see that there is no contribution to the integral from the boundary surface of the channel. We obtain, then,

$$D = \int_{S_o} (p_o + \rho U_\infty^2)\, dS_o - \int_{S_1} (p + \rho u^2) dS_1 - \int_{S_2} (p\ell + \rho u u_s) dS_2 \quad (6.6)$$

$$-\pi r_b^2\, p_b$$

A procedure for obtaining an expression for the drag as an integral extending only across the wake was suggested by Betz [6]. Let us suppose that the potential flow outside the boundary layer and wake is continued analytically into these regions. This defines a potential-flow field with velocity components u_1, v_1 and pressure p_1, which differs from the original flow field only within the boundary layer and wake. The Bernoulli equation may be applied to obtain

$$p_1 = p_0 + \frac{1}{2}\rho(U_\infty^2 - u_{1s}^2) \quad (6.7)$$

The increase in flux of fluid across the plane FG is attributable to sources bounded by the control surface of total strength

$$m = \frac{1}{4\pi} \int_{S_2} (u_{1s} - u_s) dS_2 \quad (6.8)$$

which, gives rise to a negative drag, (subscript s denotes tangential quantities)

$$D_s = -\rho \int_{S_2} U_\infty (u_{1s} - u_s) dS_2 \tag{6.9}$$

Also, we have for the flow system generating the potential flow u_1, v_1 from the momentum equation (6.5),

$$D_s = \int_{S_0} (p_0 + \rho U_\infty^2) dS_0 - \int_{S_1} (p_1 + \rho u_1^2) dS_1 - \int_{S_2} (p_1 \ell + \rho u_1 u_{1s}) dS_2$$

$$- \pi r_b^2 p_{1b} \tag{6.10}$$

where r_b is the body ordinate at the last point of calculation and p_b is the pressure on the body at this point, assumed to be constant near this region. Subtracting equation (6.10) from (6.6) gives

$$D = D_s + \int_{S_2} [(p_1 - p)\ell + \rho(u_1 u_{1s} - u u_s)] \, dS_2 + \pi r_b^2 (p_{1b} - p_b) \tag{6.11}$$

since outside S_2, $p_1 = p$, $u_1 = u$ and $v_1 = v$.

Substituting for p_1 and D_s from (6.7) and (6.9) into (6.11) gives

$$D = \ell \int_{S_2} \{(p_0 - p) + \tfrac{1}{2}\rho [U_\infty^2 - u_{1s}^2]\} dS_2$$

$$+ \rho \int_{S_2} [u_s (U_\infty - u) - u_{1s} (U_\infty - u_1)] dS_2 + \pi r_b^2 (p_{1b} - p_b) \tag{6.12}$$

an expression for the drag which involves only quantities in the boundary layer.

Now a sink of strength M is introduced in the wake on the axis v_{px} and v_{pr} are the velocity components along x and r of the net velocity due to the sink and its image system as calculated from potential theory [Ch. 3, Sec 3]. Let the quantities computed with the sink in the wake be

$$u + u^*,\ v + v^*,\ u_s + u_s^*,\ p + p^*,\ p_{1b} + p_{1b}^*,\ p_b + p_b^*$$
$$u_1 + v_{px},\ v_1 + v_{pr},\ u_{1s} + v_{ps}$$

where * indicates the small increments.

The drag in the presence of a sink can now be written as

$$D' = \ell \int_{S_2} \{(p_0 - p - p^*) + \frac{\rho}{2}[U_\infty^2 - (u_{1s} + v_{ps})^2]\} dS_2$$
$$+ \rho \int_{S_L} [(u_s + u_s^*)(U - u - u^*) - (u_{1s} + v_{ps})(U_\infty - u_1 - v_{px})] dS_2$$
$$+ \pi r_b^2 (p_{1b} + p_{1b}^* - p_b - p_b^*) \qquad (6.13)$$

Subtracting (6.12) from (6.13) and neglecting higher order terms, we obtain for the difference in drags

$$D' - D = -\ell \int_{S_L} (p^* + \rho u_{1s} v_{ps}) dS_2 + \pi r_b^2 (p_{1b}^* - p_b^*)$$
$$+ \rho \int_{S_2} [U(u_s^* - v_{ps}) + (u_{1s} v_{px} - u_s u^*)$$
$$+ (u_1 v_{ps} - u u_s^*)]\, dS_2 \qquad (6.14)$$

CHAPTER VII

DISCUSSION OF RESULTS

The drag coefficient C_D of the body based on wetted surface area, as calculated from equation (6.12), is 0.00212. This estimate is compared with the modified Squire-Young formula of Ref. [7], equation (10),

$$C_D = 2 \frac{\Delta_2}{S} \left(\frac{U_e}{U_\infty}\right)^{1/8 \left[7\left(\frac{\Delta_1}{\Delta_2} + 2\right) + 3\right]}$$

where $C_D = \frac{D}{1/2\rho U_\infty^2 S}$ is the drag coefficient based on wetted surface area S, Δ_1 is the displacement thickness, Δ_2 is the momentum thickness, U_∞ the reference velocity, U_e the velocity at the edge of the boundary layer. All the above quantities are to be evaluated at the tail of the body.

Since, in our case, the boundary-layer calculation stops before the tail of the body, the values calculated at the last station on the body are used. This should give only a small error since the last point is very close to the tail. Applying the computed values

$$\Delta_1 = 0.133832 \text{ ft}^2$$

$$\Delta_2 = 0.090478 \text{ ft}^2$$

$$\frac{\Delta_1}{\Delta_2} = 1.47917 \text{ and } \frac{U_e}{U_\infty} = 0.93226$$

$$S = 59.6588 \text{ ft}^2$$

we obtain

$$C_D = 0.00239$$

This value exceeds that from (6.12) by 12.8 percent. This discrepancy may be due to the small change in momentum thickness from the last station to the tail, which, according to Lee [3], Fig. 26.g, would decrease the above value by about 5 percent, leaving a discrepancy of about 8.5 percent.

The calculated value of the thrust deduction from the potential-flow method is 0.00021, where as the value obtained from the boundary-layer potential-flow interaction method is 0.00043. This calculation can be improved by calculating the effect due to the sink more accurately; i.e., by using a more accurate set of inputs for Green's third formula. The boundary-layer and wake equations need to be modified for a case where a singularity is present in the flow field. Also the procedure for calculating the boundary layer and wake needs to be improved so as to obtain a smooth transition from the boundary layer to the wake.

APPENDIX

To prove that the term $[\psi_d \, d\phi_o + \phi_d d\psi_o]$ is an exact differential. We have

$$\psi_d \, d\phi_o + \phi_d \, d\psi_o = \psi_d \left(\frac{\partial \phi_o}{\partial x} dx + \frac{\partial \phi_o}{\partial r} dr\right) + \phi_d \left(\frac{\partial \psi_o}{\partial x} dx + \frac{\partial \psi_o}{\partial r} dr\right)$$

$$= \left(\psi_d \frac{\partial \phi_o}{\partial x} + \phi_d \frac{\partial \psi_o}{\partial x}\right) dx + \left(\psi_d \frac{\partial \phi_o}{\partial r} + \phi_d \frac{\partial \psi_o}{\partial r}\right) dr \qquad (1)$$

The condition that this be an exact differential is that

$$\frac{\partial}{\partial r} \left(\psi_d \frac{\partial \phi_o}{\partial x} + \phi_d \frac{\partial \psi_o}{\partial x}\right) = \frac{\partial}{\partial x} \left(\psi_d \frac{\partial \phi_o}{\partial r} + \phi_d \frac{\partial \psi_o}{\partial r}\right) \qquad (2)$$

or

$$\psi_{dr} \, \phi_{ox} + \psi_d \, \phi_{oxr} + \phi_{dr} \, \psi_{ox} + \phi_d \psi_{oxr} = \psi_{dx} \, \phi_{or} + \psi_d \, \phi_{oxr} +$$

$$\phi_{dx} \, \psi_{or} + \phi_d \, \psi_{oxr}$$

or

$$\psi_{dr} \, \phi_{ox} + \phi_{dr} \psi_{ox} = \psi_{dx} \phi_{or} + \phi_{dx} \psi_{or} \qquad (3)$$

We have the following relations between the potential and stream functions in cylindrical coordinates:

$$r \frac{\partial \phi_d}{\partial r} = - \frac{\partial \psi_d}{\partial x} ; \quad r \frac{\partial \phi_o}{\partial r} = - \frac{\partial \psi_o}{\partial x}$$
$$r \frac{\partial \phi_d}{\partial x} = \frac{\partial \psi_d}{\partial r} ; \quad r \frac{\partial \phi_o}{\partial x} = \frac{\partial \psi_o}{\partial r} \qquad (4)$$

Hence, we obtain $\psi_{dr}\ \phi_{ox} = (r\ \phi_{dx})(\frac{1}{r}\ \psi_{or}) = \phi_{dx}\ \psi_{or}$ and similarly $\phi_{dr}\ \psi_{ox} = \psi_{dx}\ \phi_{or}$. By substituting these relations in (4) we realize that condition (2) is satisfied and hence $\psi_d\ d\phi_o + \phi_d\ d\psi_o$ is an exact differential.

REFERENCES

1. Huang, T.T., et al "Propeller/Sterns/Boundary-Layer Interaction on Axisymmetric Bodies: Theory and Experiment", D.T.N.S.R.D.C. Report 76-0113, December 1976.

2. Hess, J.L., and Smith, A.M.O., "Calculation of Potential Flow about Arbitrary Bodies", Progress in Aeronautical Sciences, 8, Pergamon Press, New York, 1966.

3. Lee, Y.T., "Thick Axisymmetric Turbulent Boundary Layer and Wake of a Low-Drag Body," Ph.D. Thesis, The University of Iowa, December 1978.

4. Patel, V.C., Nakayama, A., and Damian, R., "Measurements in the Thick Axisymmetric Turbulent Boundary Layer Near the Tail of a Body of Revolution," Journal of Fluid Mechanics, 63, Part 2, 1974, pp. 345-367.

5. Nakayama, A., Patel, V.C., and Landweber, L., "Flow Interaction Near the Tail of a Body of Revolution, Part 1: Flow Exterior to Boundary Layer and Wake; Part 2: Iterative Solution for Flwo Within and Exterior to Boundary Layer and Wake," Journal of Fluids Engineering, Transactions of the ASME, 98, Series 1, No. 3, September 1976.

6. Betz, A., "A Method for Direct Determination of Wing-Section Drag," Technical Memorandum No. 337, National Advisory Committee for Aeronautics, November, 1925.

7. Nakayama, A., Patel, V.C., "Calculation of the Viscous Resistance of Bodies of Revolution," IIHR Report No. 151, University of Iowa, October 1973.

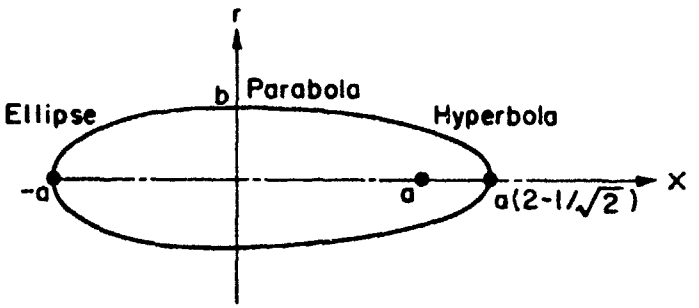

Figure 1.1 Sketch of the body of revolution

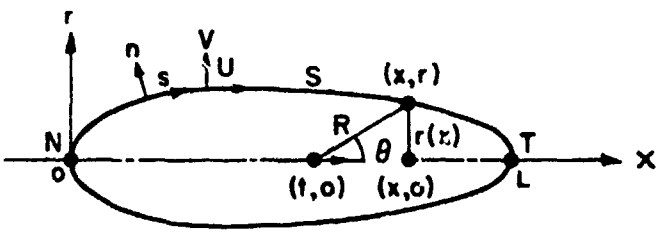

Figure 3.1 Notation for irrotational flow outside the closed body

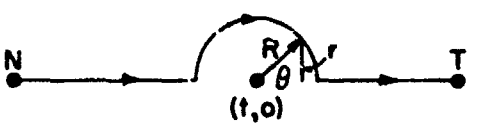

Figure 3.2 Path of integration for equation (3.7)

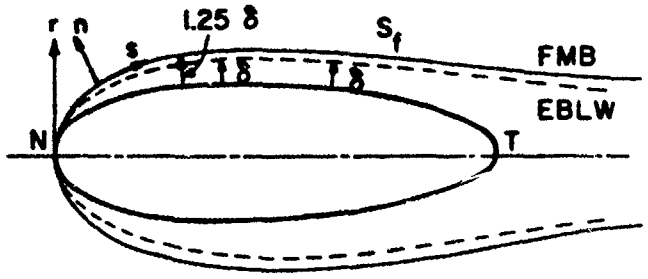

Figure 3.3 Definition sketch showing the fixed matching boundary enclosing the edge of boundary-layer and wake

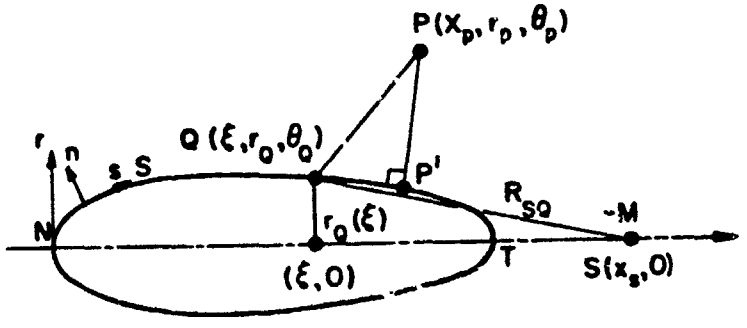

Figure 3.4 Notation for equation (3.18)

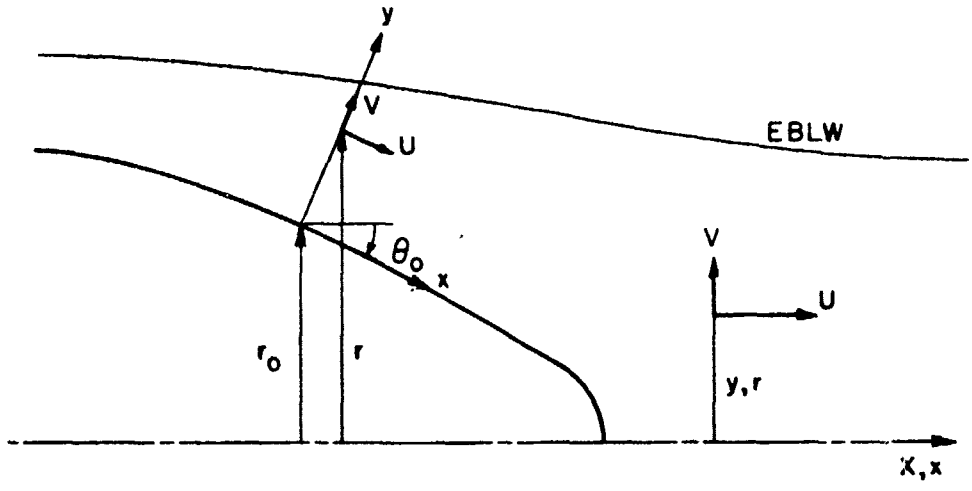

Figure 4.1 Definition sketch for boundary layer equations

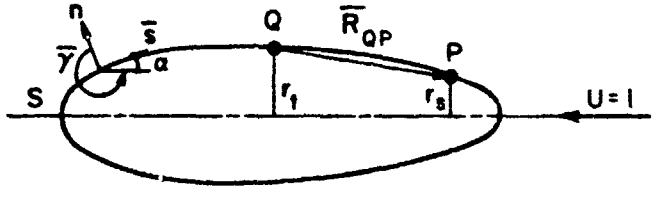

Figure 6.1 Notation for equation (6.2)

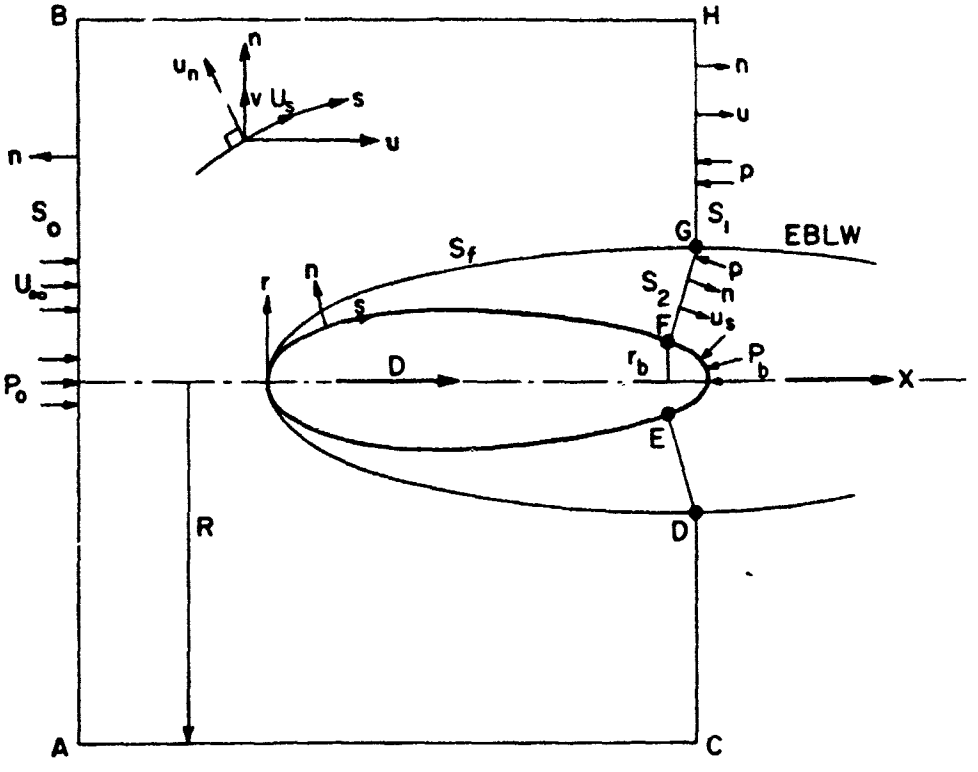

Figure 6.2 Control volume for the calculation of drag